A search for $\nu_\mu \rightarrow \nu_\mathrm{e}$ oscillations in the MINOS experiment

J.J. Evans (for the MINOS collaboration)
Department of Physics and Astronomy, University College London, Gower Street, London, WC1E 6BT, United Kingdom

Abstract
The MINOS experiment uses the NuMI neutrino beam to make precision measurements of the neutrino mixing parameters. A beam of ν_μ is produced at Fermilab. Its energy spectrum is measured near the production point, and again after 735 km at the Soudan Underground Laboratory. By looking for ν_e appearance in the beam, limits can be placed on the as yet unmeasured mixing angle θ_{13}. At the far detector (in the Soudan laboratory), 35 ν_e candidate events are observed with a predicted background of $27 \pm 5(\mathrm{stat.}) \pm 2(\mathrm{syst.})$ events: a 1.5σ excess. At 90% C.L. this gives an upper limit range of $\sin^2(2\theta_{13}) < 0.28$–$0.34$ for the normal neutrino mass hierarchy and $\sin^2(2\theta_{13}) < 0.36$–$0.42$ for the inverted hierarchy, depending upon the CP-violating phase δ_CP.

1 The MINOS experiment

The MINOS experiment uses the NuMI ν_μ beam, produced from 120 GeV protons at the Fermilab accelerator complex in Chicago. The beam consists of 98.7% $\nu_\mu + \overline{\nu}_\mu$ and 1.3% $\nu_\mathrm{e} + \overline{\nu}_\mathrm{e}$. The neutrino energy spectra are measured at the near detector (ND), 1 km from the source, before oscillations have had time to occur. They are then measured again at the far detector (FD), 735 km from the source at the Soudan Underground Laboratory in northern Minnesota. Comparing the energy spectra at the two detectors allows the relevant oscillation parameters to be measured.

The two detectors are of similar design to reduce systematic uncertainties due to neutrino interaction physics, beam flux and detector response. They are tracking, sampling calorimeters consisting of alternate planes of 2.54 cm-thick steel and 1 cm-thick scintillator strips of 4 cm width [1].

If θ_{13} is non-zero a small fraction of ν_μ will oscillate to ν_e. If θ_{13} is at the Chooz limit [2], MINOS can detect this ν_e appearance to make the first measurement of a non-zero θ_{13}. At $\sin^2(2\theta_{13}) = 0.15$, 11 signal and 27 background events would be observed. The ν_e appearance probability for MINOS is

$$P(\nu_\mu \rightarrow \nu_\mathrm{e}) = \sin^2(2\theta_{13}) \sin^2(\theta_{23}) \sin^2\left(\frac{\Delta m^2_{\mathrm{atm}} L}{4E}\right) \qquad \text{(to leading order).}$$

2 Electron neutrino event selection

The MINOS detectors are optimized for the identification of charged current (CC) interactions of muon-type neutrinos and neutral current (NC) interactions of any neutrino flavour. They are therefore designed for muon tracking and hadronic shower calorimetry. The signal for this analysis is the CC interaction of electron neutrinos, producing an electromagnetic (e.m.) shower in the detector, characterized by a denser energy deposition near the event vertex than in a hadronic shower. The detector granularity is not optimal for distinguishing e.m. from hadronic showers: for e.m. showers, the radiation length in steel is 1.76 cm, compared to the 2.54 cm steel thickness; the Molière radius is 3.7 cm, compared to the 4.1 cm scintillator strip width. A typical 2 GeV ν_e-CC event covers 8 planes and 4 strips.

A number of preselection cuts are used to reduce the NC and ν_μ-CC backgrounds:

- The length of any track must be less than 25 planes.
- The number of track-only planes must be fewer than 16.

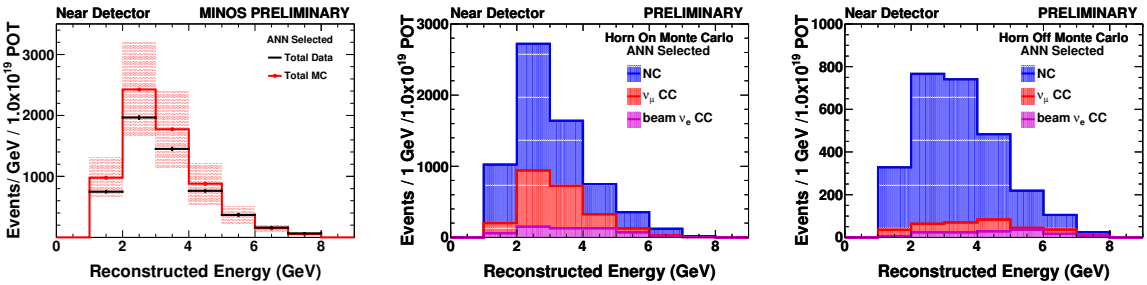

Fig. 1: Left: the reconstructed energy spectrum of ν_e-CC-like events at the near detector, comparing data (black) and simulation (red, with systematic error shown as the light red band). Centre: the composition of the sample with the NuMI beam focusing horns switched on; right: the composition with the focusing horns switched off.

– The reconstructed energy of the event must be between 1 GeV and 8 GeV.
– The event must contain at least one shower with more than four contiguous planes and greater than 0.5 MIP (minimum ionizing particle) of energy deposition.

This preselection takes the signal to background ratio to 1:12 from 1:55 (assuming $\sin^2(2\theta_{13}) = 0.15$).

A more sophisticated selection algorithm is required to further improve the sample purity. To do this, variables are formed which characterize the shower shape, length and width. Eleven such variables are combined into an artificial neural network (ANN) [3], shown in figure 2. This takes the signal:background ratio to 1:4 (for $\sin^2(2\theta_{13}) = 0.15$) with a signal efficiency of 41%, NC rejection power of 92.3% and ν_μ-CC rejection power of 99.4%.

3 Background correction

The ν_e-selected ND data and simulation disagree by up to 20%, as shown in figure 1. This is expected, since the selection cuts hard to reduce backgrounds, leaving only tails of distributions. The two-detector nature of MINOS means the ND data can be used to correct for these discrepancies in the FD simulation.

The ν_e sample is made up of a number of background components, primarily NC and ν_μ-CC events, which must be corrected independently. By turning off the current in the NuMI beam focusing horns, the relative background contributions change in a well-modeled way, as shown in figure 1, allowing the individual components to be measured. After this correction the background consists of $(57\pm5)\%$ NC, $(32 \pm 7)\%$ ν_μ-CC and $(11 \pm 3)\%$ from CC interactions of the intrinsic ν_e beam background.

These background corrections are applied to the far detector simulation to give a total systematic uncertainty of 7.3% on the number of selected events, compared to a statistical uncertainty of 19%. An independent method of correcting the background takes the well-understood ν_μ-CC events and removes the muon from the reconstructed event to leave a well-understood sample of hadronic showers [4]. This produces consistent results.

4 Results

At the far detector, 35 ν_e-CC candidate events are seen. The expected background is 27 ± 5(stat.)±2(syst.) events. This is an excess of 1.5σ. The distribution of the selection variable (ANN) for these events is shown in figure 2, along with the reconstructed energy spectrum.

The best fit value for $\sin^2(2\theta_{13})$ is at the Chooz limit, and is dependent on the mass hierarchy (sign of $\Delta m^2_{\rm atm}$) and the CP-violating phase $\delta_{\rm CP}$. There is also a dependence on the values of $\sin^2(2\theta_{23})$ and $\Delta m^2_{\rm atm}$. All values quoted assume the MINOS best fit value of $\Delta m^2_{\rm atm} = 2.43 \times 10^{-3}\,{\rm eV}^2$ and $\sin^2(2\theta_{23}) = 1.0$ [5].

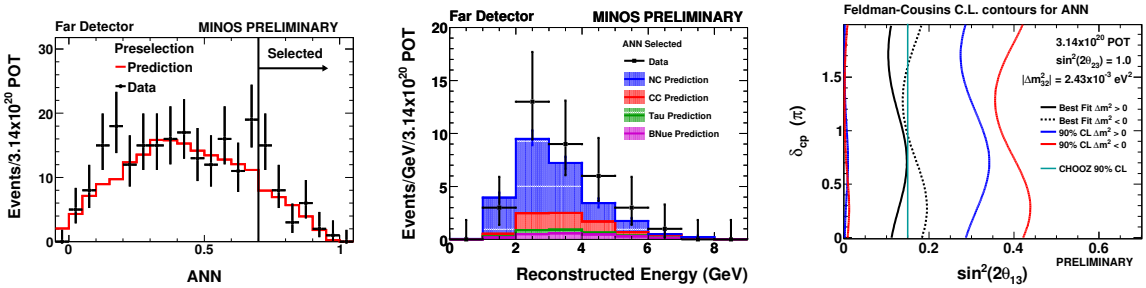

Fig. 2: Left: the distribution of the ν_e selection variable (ANN) for the far detector data (black), compared to the simulation after background correction (red); events to the right of the vertical black line are selected as ν_e-CC-like. Centre: the reconstructed energy spectrum of the selected ν_e-CC-like events in the far detector (black crosses), compared to the simulation after background correction (coloured, filled histograms) assuming $\theta_{13} = 0$. The various colours show the contributions from different backgrounds. Right: the MINOS 90% C.L. allowed regions for $\sin^2(2\theta_{13})$ for the normal (blue) and inverted (red) mass hierarchies. Also shown are the MINOS best fit values (black) and the Chooz 90% confidence limit [2] (grey).

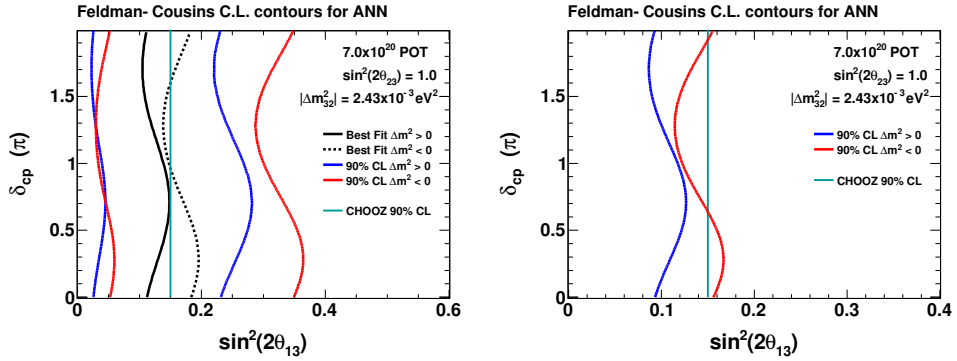

Fig. 3: The sensitivity of MINOS to $\sin^2(2\theta_{13})$ for an exposure of 7×10^{20} protons on target under two assumptions: left, that the observed excess persists in the new data; right, that there is no excess in the new data.

The 90% C.L. allowed regions for $\sin^2(2\theta_{13})$ are shown in figure 2. Assuming $\delta_{\rm CP} = 0$, MINOS allows $\sin^2(2\theta_{13}) < 0.29$ (90% C.L.) for the normal mass hierarchy, and $\sin^2(2\theta_{13}) < 0.42$ (90% C.L.) for the inverted hierarchy.

5 The future

The results presented here correspond to an exposure of 3.2×10^{20} protons on target (PoT). As of June 2009, MINOS has more than doubled this dataset, obtaining 7×10^{20} PoT. In early 2010, the analysis will be updated to include this new data. Figure 3 shows the sensitivity to $\sin^2(2\theta_{13})$ for this increased dataset, depending on whether the observed excess persists or goes away in the new data.

References

[1] D.G. Michael *et al.*, Nucl. Instrum. and Meth. **A596**, 190 (2008).

[2] M. Apollonio *et al.*, Eur. Phys. J. **C27**, 331 (2003).

[3] T. Yang, Ph.D. Thesis, Stanford University (2009).

[4] A. Holin, Ph.D. Thesis, UCL (2009).

[5] P. Adamson *et al.*, Phys. Rev. Lett. **101**, 131802 (2008).